Available online at www.sciencedirect.com
ScienceDirect
Radiation Measurements 43 (2008) 1343–1353
Radiation Measurements
www.elsevier.com/locate/radmeas

Simulations of the predose technique for retrospective dosimetry and authenticity testing

V. Pagonis*, E. Balsamo, C. Barnold, K. Duling, S. McCole

Physics Department, McDaniel College, Westminster, MD 21158, USA

Received 25 March 2008; received in revised form 23 April 2008; accepted 30 April 2008

Abstract

The predose technique of thermoluminescence (TL) for quartz has been used extensively for retrospective dosimetry and archaeological authenticity testing. In this paper, we use a previously published comprehensive kinetic model for quartz, to simulate the complete sequence of experimental steps taken during the additive dose and the multiple activation versions of the predose technique. The simulation results show how both versions of the predose technique can reproduce the paleodose received by the sample with an accuracy of 1–5% in the low dose region of 0–2 Gy. For doses greater than ~ 2 Gy the non-linear dose dependence of the sensitivity of the "110 °C" TL peak causes significant inaccuracies in the technique. The solution of the kinetic differential equations elucidates several electron and hole processes taking place during the experimental predose procedure; these processes include the thermal transfer of holes from the Zimmerman hole reservoirs to the luminescence center, the radiation quenching of the TL sensitivity and the radiation-enhanced sensitivity of quartz samples. Specific numerical examples are given for samples exhibiting the thermal activation characteristics of "low-S_0" and "high-S_0" values. Quantitative results are presented for the effect of the test dose and of the calibration beta dose β on the accuracy of both versions of the predose technique. Results are also presented for the sensitivity of the predose technique to the natural variations of the hole concentrations in the luminescence center. Finally, the results of the predose technique simulations are compared with those from simulating the popular single aliquot SAR/OSL technique based on optically stimulated luminescence signals.

Keywords: Thermoluminescence; Predose effect; Quartz; Retrospective dosimetry; Authenticity testing; Accident dosimetry; Quartz annealing; Kinetic rate equations; Additive dose method; Multiple activation method

1. Introduction

The predose technique is a well-established experimental method for determining the total cumulative dose from natural radiation sources, for accident dosimetry and for archaeological authenticity testing (Aitken, 1985; Bailiff, 1994, 1997; and references therein). The method is based on the observed change of sensitivity of the "110 °C" thermoluminescence (TL) peak of quartz, caused by a combination of irradiation and high temperature annealing. The range of doses that can be estimated using the predose technique has been shown to range from a few tens of mGy, to larger doses of the order of several Gy, with the upper limit restricted by the early onset of saturation. The predose technique has been used successfully for retrospective and accident dosimetry (Bailiff and Haskell, 1984; Haskell et al., 1988, 1994; Haskell, 1993; Hütt et al., 1993). In more recent work, it was shown that the 210 °C peak of quartz and porcelain exhibited similar characteristics to the 110 °C TL peak, and that the combined use of the two peaks can be used to estimate small accrued doses in several types of materials (Bailiff and Haskell, 1984; Stoneham, 1985; Göksu et al., 1998, 2001; Bailiff and Holland, 2000; Bailiff et al., 2000; Galli et al., 2006). Several explanations of the predose effect have been proposed which are based on specific impurities in quartz crystals (Martini et al., 1987; Yang and McKeever, 1988; Itoh et al., 2001).

Although the predose technique is well established experimentally, further theoretical and modeling work is needed in order to obtain a better understanding of the complex predose mechanism. There have been several published theoretical studies of the predose technique in the literature.

* Corresponding author. Tel.: +1 410 857 2481; fax: +1 410 386 4624.
E-mail address: vpagonis@mcdaniel.edu (V. Pagonis).

1350-4487/$ - see front matter © 2008 Elsevier Ltd. All rights reserved.
doi:10.1016/j.radmeas.2008.04.095

Zimmerman (1971a,b) first proposed a predose model consisting of one electron trapping state T, a luminescence center L and a hole reservoir. Chen (1979) proposed a modification of the Zimmerman model by adding an extra electron level S which competes for electrons during the heating stage. By using physical arguments concerning the observed experimental behavior of quartz samples, Chen and Leung (1998, 1999) introduced a modified version of the Zimmerman model and successfully explained the linear dependence of the TL signal on the test dose, the exponential approach of the sensitivity to saturation with repeated additive doses and the phenomena of radiation quenching, UV reversal and the distinction between reservoir and center saturations. The model has also been used to describe the experimentally observed superlinearity of predosed and annealed quartz samples (Pagonis et al., 2003; Polymeris et al., 2006).

Recently, Kitis et al. (2006a,b) presented a broad study of the predose effect and the thermal-activation characteristics of three quartz samples of different origin. The thermal-activation characteristics were measured as a function of several experimental parameters using both multiple-aliquot and single-aliquot techniques, and complete TL vs. dose and sensitivity S vs. predose curves were obtained for the dose range of $0.1 < D < 400$ Gy. The results of this experimental study for all three quartz samples were interpreted by using a simple modified Zimmerman model for quartz consisting of two electron traps, a luminescence center and three hole reservoirs. Pagonis et al. (2006) simulated the sensitization of quartz samples as a function of the annealing temperature, yielding the so-called thermal activation characteristic (TAC). These authors also used a modified Zimmerman model to simulate multiple TACs and the effect of UV-radiation on the TL sensitivity of quartz; these phenomena are important analytical and diagnostic tools during applications of the predose technique. Adamiec et al. (2004, 2006) presented a comprehensive kinetic model for the predose effects in quartz, consisting of three non-radiative recombination centers and one radiative center, as well as two electron traps and a reservoir electron trap. The model successfully simulated the experimentally observed thermal activation characteristics and isothermal sensitization of quartz samples.

Pagonis and Carty (2004) used a modified version of the model by Chen and Leung (1998, 1999) to simulate the complete sequence of experimental steps taken during the additive dose version of the predose technique. Their simulation results showed that the additive dose technique can reproduce accurately the accumulated dose or paleodose (PD) received by the sample with an accuracy of ±1–5% over several orders of magnitude of the paleodose.

The purpose of the present paper is to simulate the complete sequence of experimental steps taken during the predose technique, using the comprehensive quartz model developed by Bailey (2001). These new simulations extend our previous work to include a description of the multiple activation version of the predose technique, as well as a comparison with the popular single aliquot regenerative technique (SAR/OSL), which is based on optically stimulated luminescence (OSL) signals. To the best of our knowledge, the complete sequence of events in the two versions of the predose technique has not been simulated numerically before. The present simulations also demonstrate the phenomenon of radiation quenching and its effects on the results of the predose technique.

2. Description of the model

The simulations in this paper are carried out using the comprehensive quartz model developed by Bailey (2001) on the basis of empirical data. The model has been successful in simulating several TL and OSL phenomena in quartz (Bailey, 2001; Pagonis et al., 2007a, b). Fig. 1 shows the energy level diagram in the model; the four energy levels denoted by 1, 6, 7 and 8 in Fig. 1 play a fundamental role in the predose phenomenon. For the sake of completeness, we provide a brief description of the different energy levels in the model.

Level 1 in the model represents the 110 °C TL shallow electron trap, which gives rise to a TL peak at ∼ 100 °C when measured with a heating rate of $5\,\mathrm{K\,s^{-1}}$. This TL peak has been the subject of numerous studies because of its importance in predose dating (Bailiff, 1994) and retrospective dosimetry (Bailiff, 1994, 1997). Level 2 represents a generic "230 °C TL level", typical of such TL peaks found in many sedimentary quartz samples. Levels 3 and 4 are usually termed the fast and medium OSL components (Bailey et al., 1997) and they yield TL peaks at ∼ 330 °C as well as giving rise to OSL signals. Level 5 is a deep, thermally disconnected, electron center. Such a level is known to be necessary in order to explain several TL and OSL phenomena based on competition between energy levels. The model contains also four hole trapping centers (levels 6–9) which act as recombination centers for optically or thermally released electrons. Levels 6 and 7 are thermally unstable, non-radiative recombination centers, similar to the "hole reservoirs" first introduced by Zimmerman (1971a,b) in order to explain the predose sensitization phenomenon in quartz. Level 8 is a thermally stable, radiative recombination center termed the "luminescence center" (L in the Zimmerman model). Holes can be thermally transferred from the two hole reservoirs (levels 6 and 7) into the luminescence center via the valence band. Level 9 is a thermally stable, non-radiative recombination center termed a "killer" center (K in the Zimmerman model).

In the current study, the computer code is written in *Mathematica*, and the parameters are as defined by Bailey (2001); N_i are the concentrations of electron traps or hole centers ($\mathrm{cm^{-3}}$), n_i are the concentrations of trapped electrons or holes ($\mathrm{cm^{-3}}$), s_i are the frequency factors (per second, $\mathrm{s^{-1}}$), E_i are the electron trap depths below the conduction band or hole center energy levels above the valence band (eV), A_i are the valence band to trap transition probability coefficients ($\mathrm{cm^3\,s^{-1}}$) and B_i are the conduction band to hole center transition probability coefficients ($\mathrm{cm^3\,s^{-1}}$). Other parameters used in the model are the photo-eviction constant θ_{0i} ($\mathrm{s^{-1}}$) at $T = \infty$, the thermal assistance energy E_i^{th} (eV) and the photon stimulation flux P. The parameters n_c and n_v represent the instantaneous concentrations of electrons and holes in the conduction and valence band correspondingly.

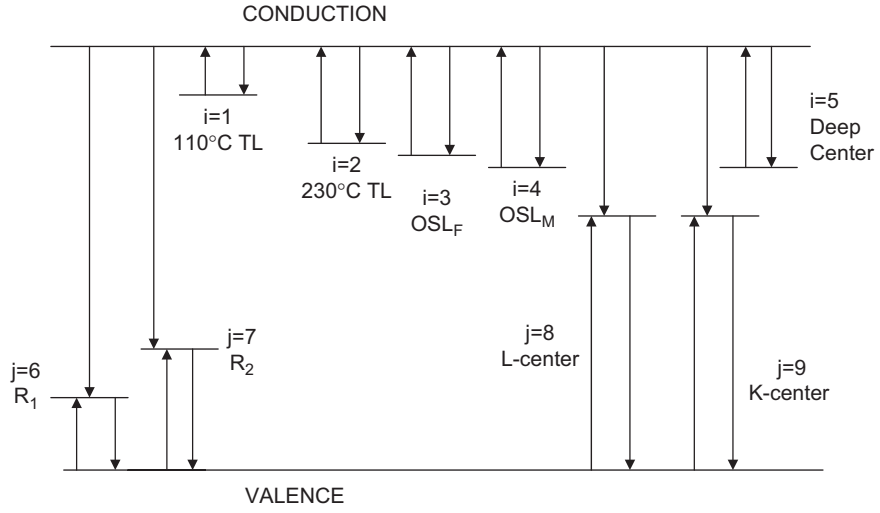

Fig. 1. Schematic diagram of the comprehensive Bailey (2001) model for quartz.

Table 1
The simulation steps for the thermal activation characteristic (TAC) of a quartz sample

1.	Natural sample. All electron and hole concentrations set to zero.
2.	Natural Irradiation with a paleodose of 1 Gy with the slow natural dose rate of 10^{-11} Gy s^{-1}.
3.	The sample is given a beta dose of 10 Gy in the laboratory.
4.	The sample is heated to the activation temperature (in the range 20–600 °C).
5.	Give test dose TD = 0.1 Gy. Measure TL sensitivity S_N by heating to 150 °C.
6.	Repeat steps 3–6 using a higher activation temperature.

Table 2
The simulation steps for the additive dose version of the predose technique

1.	Natural sample. All electron and hole concentrations set to zero.
2.	Natural Irradiation with a paleodose β with the slow natural dose rate of 10^{-11} Gy s^{-1}.
3.	Give test dose, usually 0.01 Gy. Measure initial sensitivity S_0 using the 110 °C TL peak.
4.	Heat to 500 °C.
5.	Give Test Dose. Measure S_N.
6.	Use a new aliquot; give test dose. Measure S_0.
7.	Give calibration dose β.
8.	Heat to 500 °C.
9.	Give test dose. Measure $S_{N+\beta}$.
10.	Repeat steps 6–10 using doses of 2β, 3β, etc. in step 7, to obtain the sensitivities $S_{N+2\beta}$, $S_{N+3\beta}$, etc. Obtain the graph of the sensitivity S vs. added dose, as shown in Fig. 4a.

The equations used in this study are as follows:

$$\frac{dn_i}{dt} = n_c(N_i - n_i)A_i - n_i P\theta_{oi}\, e^{(-E_i^{th}/k_B T)} - n_i s_i\, e^{(-E_i/k_B T)} \quad (i = 1, \ldots, 5) \tag{1}$$

$$\frac{dn_j}{dt} = n_v(N_j - n_j)A_j - n_j s_j e^{(-E_j/k_B T)} - n_c n_j B_j \quad (j = 6, \ldots, 9) \tag{2}$$

$$\frac{dn_c}{dt} = R - \sum_{i=1}^{5}\left(\frac{dn_i}{dt}\right) - \sum_{j=6}^{9}(n_c n_j B_j) \tag{3}$$

$$\frac{dn_v}{dt} = \frac{dn_c}{dt} + \sum_{i=1}^{5}\left(\frac{dn_i}{dt}\right) - \sum_{j=6}^{9}\left(\frac{dn_j}{dt}\right) \tag{4}$$

The luminescence is defined as

$$L = n_c n_8 B_8 \eta(T) \tag{5}$$

with $\eta(T)$ representing the luminescence efficiency, and R denoting the pair production rate. Within the model, a value of $R = 5 \times 10^7$ cm^{-3} s^{-1} corresponds to a beta dose rate of 1 Gy s^{-1} in the laboratory (Bailey, 2001, footnote p. 22). An important improvement of the present simulations over the work of Pagonis and Carty (2004) is the use of appropriate units of dose to express the paleodoses of the quartz samples. Pagonis

Table 3
The simulation steps for the multiple activation version of the predose technique

1.	Natural sample. All electron and hole concentrations set to zero.
2.	Natural Irradiation with a paleodose β with the slow natural dose rate of 10^{-11} Gy s^{-1}.
3.	Give test dose (TD). Measure S_0.
4.	Heat to 500 °C.
5.	Give test dose (TD). Measure S_N.
6.	Give calibration dose β.
7.	Heat to 150 °C to empty the traps.
8.	Give Test Dose (TD). Measure $S_{N'}$.
9.	Heat to 500 °C.
10.	Give test dose (TD). Measure $S_{N+\beta}$.
11.	Calculate accrued dose AD using S_0, S_N, $S_{N+\beta}$ and $S_{N'}$ in Eqs. (6) and (7).
12.	Find percent difference of PD and AD.

A single aliquot is used for all measurements.

Table 4
The simulation steps for the OSL/SAR technique

1.	Natural sample. All electron and hole concentrations set to zero.
2.	Natural Irradiation with a paleodose β with the slow natural dose rate of 10^{-11} Gy s^{-1}.
3.	Irradiate sample with dose D_i.
4.	Preheat 10 s at 260 °C.
5.	Blue OSL for 100 s—record OSL (0.1 s) signal (L).
6.	Test dose TD = 0.1 Gy.
7.	Cutheat 20 s at 220 °C.
8.	Blue OSL for 100 s—record OSL (0.1 s) signal (T).
9.	Repeat steps 3–8 for the sequence of doses 0.8β, β, 1.2β, 0 and 0.8β to reconstruct the dose response curve L/T vs. dose. Calculate the accrued dose AD using interpolation.

A single aliquot is used for all measurements.

and Carty (2004) presented their paleodoses in units of cm^{-3}, while the present work uses appropriate units of Gy instead.

As discussed in Bailey (2001), the ionization rate (cm^{-3} s^{-1}) depends on the exact experimental conditions, namely the strength of the source and on the geometry used during irradiation of the sample. The choice of the R value in the Bailey (2001) model is more or less arbitrary, and was chosen so that the simulated TL and OSL results are similar to common experimental TL and OSL data for quartz.

Table 1 shows in schematic form the steps simulated in the computer program for a typical measurement of the thermal activation characteristic (TAC) of a quartz sample. Table 2 shows the corresponding simulation steps for the additive dose version of the predose technique, and Table 3 shows the steps taken during application of the multiple activation version. Finally, Table 4 contains the steps in simulating the SAR/OSL technique for quartz.

After each excitation stage in the simulations a relaxation period is introduced in which the temperature of the sample is kept constant at room temperature for 1 s after the excitation has stopped ($R = 0$), and the concentrations of n_c, n_v decay to negligible values. After each heating cycle to 150 or 500 °C, the model simulates a cooling-down period with a constant cooling rate of $\beta = -5$ °C s^{-1}. A linear heating rate $\beta = 5$ °C s^{-1} is assumed during the measurement of the TL glow curves, so that $T = T_0 + \beta t$ and $R = 0$ during the readout stage.

3. Simulation of the thermal activation characteristic (TAC) of the quartz sample

Before application of the predose technique it is necessary to measure the sensitivity of the quartz sample to a small beta dose, after heating the sample to a progressively increasing activation temperature. This type of measurements is known as a thermal activation characteristic (TAC) of the quartz sample. Table 1 shows the simulation steps of the thermal activation characteristic (TAC) of a quartz sample. In the first step of Table 1 the concentrations of all traps are set to zero, while in step 2 the sample is given a paleodose of 1 Gy. In order to simulate the natural dose rate as close as possible, a dose rate of 10^{-11} Gy s^{-1} is used during the natural irradiation of the sample in step 2 (Bailey, 2004). In step 3 the sample is given a beta dose of 10 Gy in the laboratory, and in step 4 it is heated to the activation temperature (in the range 20–600 °C).

In step 5 the sample is given a small beta test dose (TD) of 0.1 Gy and is heated to 150 °C to measure the sensitivity S_N, which is represented by the maximum of the TL peak at 110 °C. The whole process is repeated in step 6 by re-irradiating the sample with 10 Gy and using a higher activation temperature each time, thus obtaining the variation of the sensitivity S_N with the activation temperature. The results of simulating such a TAC measurement sequence are shown in Fig. 2a for three different values of the total concentration of holes N_8 in the luminescence center. The value of N_8 is varied over three orders

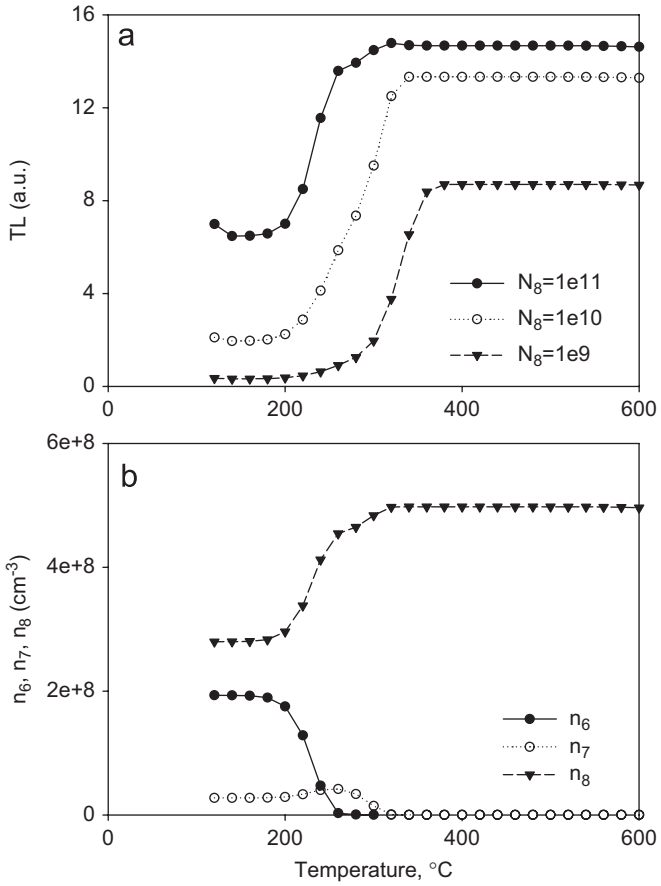

Fig. 2. (a) Simulated thermal activation characteristic (TAC) for quartz for three different values of the concentration N_8 of the luminescence center. The various steps in the simulation are described in the text. (b) The variation of the concentration of hole centers n_6, n_7 and luminescence center n_8 with the annealing temperature, showing the transfer of holes from the Zimmerman reservoirs to the luminescence center L.

of magnitude, from the original large value of $N_8 = 10^{11}\,\mathrm{cm}^{-3}$ in the Bailey model, to a much reduced value of $N_8 = 10^9\,\mathrm{cm}^{-3}$.

For a 5-mg sample of quartz, a typical increase of the sensitivity is around 2–10 times for a predose of 1 Gy (Aitken, 1985, p. 155). In practical applications it is desirable to have a value of the room temperature sensitivity S_0 many times smaller than the thermally activated sensitivity S_N. This is known as the requirement of "low-S_0" values for accurate application of the predose technique.

The top graph in Fig. 2a represents the TAC simulated using the original Bailey parameters (with $N_8 = 10^{11}\,\mathrm{cm}^{-3}$), and shows an increase of the sensitivity from a value of $S_0 \sim 6$ at low temperatures, up to the thermally activated value of $S_N \sim 15$. The activation ratio in this case is only $S_N/S_0 \sim 2.5$ and this can be considered representative of a sample exhibiting a "high-S_0" value. The bottom graph in Fig. 2a represents the TAC simulated using the much smaller value of $N_8 = 10^9\,\mathrm{cm}^{-3}$ and shows an increase of the sensitivity from a value of $S_0 \sim 0.4$ at low temperatures, up to the thermally activated value of $S_N \sim 8.5$. The activation ratio in this case is much larger $S_N/S_0 \sim 21$ and this can be considered representative of a sample exhibiting a "low-S_0" value. In the rest of this paper, we will present mostly numerical results for a sample exhibiting "low-S_0" value by using a value of the parameter $N_8 = 10^9\,\mathrm{cm}^{-3}$. Some results comparing the glow curves of samples with low-S_0 and high-S_0 values are presented later in the paper.

Fig. 2b shows the concentrations of holes $n_8(T)$ in the luminescence center L and $n_6(T)$, $n_7(T)$ in the hole reservoirs R_1 and R_2 correspondingly, as a function of the annealing temperature T during the TAC simulation. The results of Fig. 2b show that the model successfully describes the predose activation process, which consists of the hole transfer from R_1 and R_2 to L during the heating of the sample to 400–600 °C. As the temperature T increases, the concentration of holes $n_8(T)$ in the luminescence center L is increased, while the corresponding concentrations of holes $n_6(T)$ and $n_7(T)$ in the Zimmerman hole reservoirs R_1 and R_2 are decreased by the same total amount. The results of Fig. 2a and b also show that an activation temperature in the region 400–600 °C is sufficiently high to transfer all holes from the Zimmerman hole reservoirs R_1 and R_2 into the luminescence center L. The exact shape of the TAC and the optimal value of the activation temperature depend on the experimental details of the measurement, and have been the subject of a separate theoretical study presented elsewhere (Chen and Pagonis, 2004).

4. The additive dose variation of the predose technique

Two main variations of the predose technique exist, known as the multiple thermal activation technique and the additive dose technique. In a typical experimental application of the predose procedure, a test dose TD = 0.01 Gy is commonly used, as well as a calibration dose β with a value close to the estimated paleodose of the sample. The exact value of the calibration dose to be used in the experiment is usually found by trial and error. The response to the test dose TD is measured by heating the sample to 150 °C, just above the "110 °C" TL peak. The basic sequence of measurements during the additive dose technique is shown in Table 2 and is based on the use of several aliquots of the sample (Aitken, 1985, pp. 153–168). Steps 1 and 2 in Table 2 are identical to the corresponding steps during the TAC simulation in Table 1, except that the sample receives a paleodose (PD) of β Gy in step 2. Using the first portion of the material the TL sensitivities S_0 and S_N to a small test dose (TD) are measured as shown in steps 3–5 of Table 2. Using the remaining portions of the material, the TL sensitivities of the irradiated samples $S_{N+\beta}$, $S_{N+2\beta}$, $S_{N+3\beta}$, etc. are measured as shown in steps 6–10 of Table 2.

The additive dose variation of the predose technique avoids multiple thermal activation of the material, which can cause changes to its pre-dose characteristics. It also avoids complications arising from the phenomenon of radiation quenching, which is described in the next section. The obvious disadvantage of the additive dose technique is the need for inter-calibration between the different aliquots. Such inter-calibration can typically add additional inaccuracies of a few percent to the estimated value of the accrued dose in the sample. In practice,

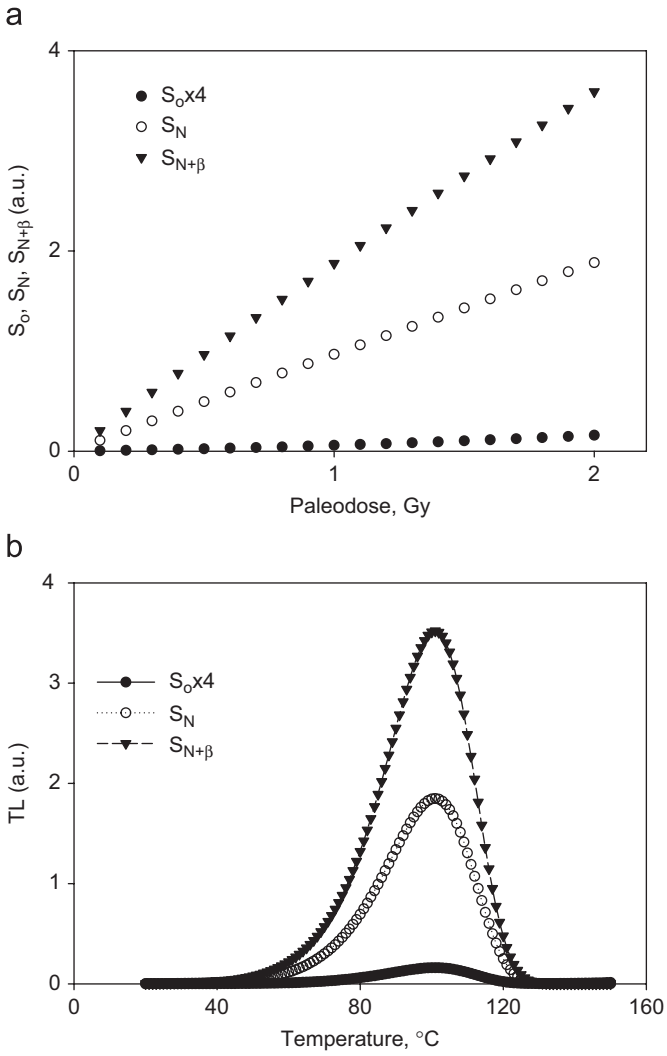

Fig. 3. Simulation results for the additive dose version of the predose technique. (a) The linear variations of the sensitivities S_0, S_N, $S_{N+\beta}$ with the paleodose PD, as calculated by the model in the range 0–2 Gy. (b) Simulated glow curves for the additive dose technique with the test dose TD = 0.01 Gy, a paleodose PD = 4 Gy, a calibration beta dose of 4 Gy and an activation temperature of 500 °C.

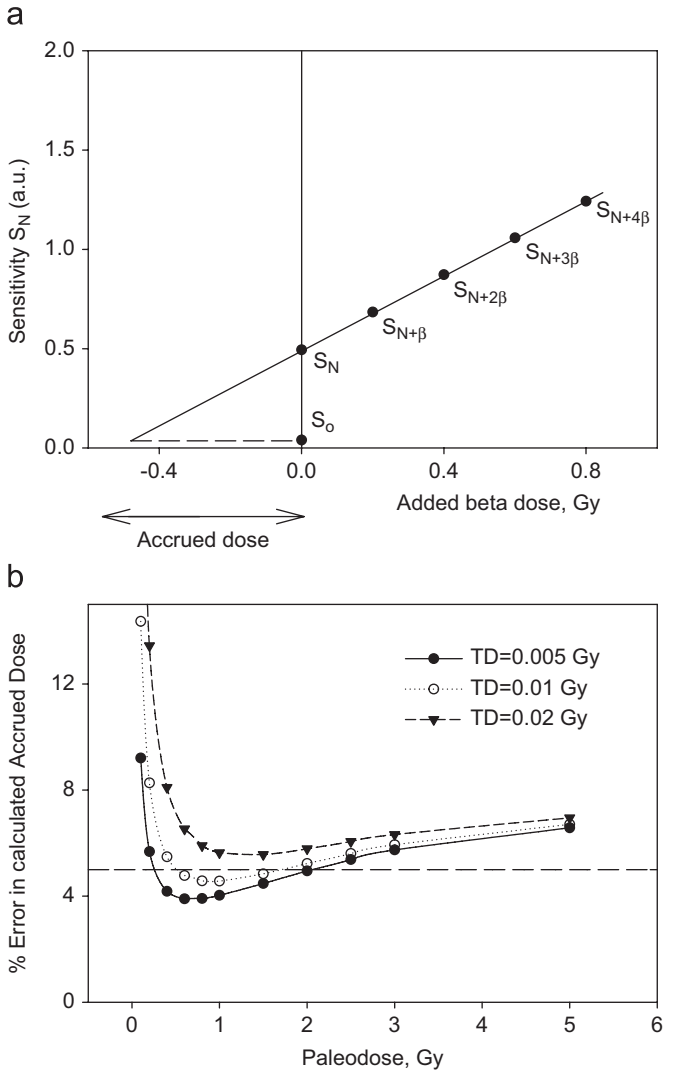

Fig. 4. (a) The simulated variation of the sensitivity S of the 110 °C TL peak with the added beta dose. Extrapolation on the x-axis gives the estimated accrued dose (AD) of the sample as shown. (b) The variation of the accuracy of the calculated accrued dose (AD) with the paleodose PD and for three different values of the test dose TD. A fixed calibration dose $\beta = PD$ is used in this simulation.

normalization using the weight of the samples does not give good precision, and one can use the S_0-value of the samples for normalization purposes. However, this cannot be done reliably for samples exhibiting the desirable low S_0-value (Aitken, 1985, p. 163).

The dose evaluation in the additive dose technique is based on the assumption of a linear variation of the sensitivity of the sample with the dose, which is shown in Fig. 3 and is discussed in a subsequent section. By extrapolating the graph of the sensitivity S to the dose axis as shown in Fig. 4a, one obtains an estimate of the accrued dose (AD) of the sample. The simulation in Table 2 calculates the percent difference between the calculated accrued dose (AD) and the known value of the paleodose (PD) using the extrapolation procedure shown in Fig. 4a, for a wide range of paleodoses. The result is shown in Fig. 4 and is discussed in Section 6.

5. The multiple activation variation of the predose technique

The basic sequence of measurements during the multiple activation technique is shown in Table 3 and is based on the use of a single aliquot of the sample (Aitken, 1985, pp. 153–168). The TL sensitivities S_0 and S_N of the material to a small test dose (TD) are measured as shown in steps 3–5 of Table 3. The thermally activated sensitivities $S_{N+\beta}$ and $S_{N'}$ are measured using the same aliquot as shown in the rest of Table 3.

Experiments using the multiple activation variation exhibit the phenomenon of radiation quenching. This phenomenon consists of the sensitivity $S_{N'}$ in step 8 being usually lower than the sensitivity S_N in step 5, due to the beta irradiation in step 6 of Table 3. In addition, in this technique the aliquot undergoes a multiple thermal activation, which can cause changes to

its pre-dose characteristics. The equations used in the multiple activation technique are also based on the assumption of a linear response of the sensitivity of the sample. The accrued dose (AD) can be calculated using the equation:

$$\mathrm{AD} = \frac{S_N - S_o}{S_{N+\beta} - S_N} \times \beta \tag{6}$$

When the effect of radiation quenching is taken into account, Eq. (6) is modified by using the quenched sensitivity $S_{N'}$ instead of the sensitivity S_N, to obtain a corrected estimate of the accrued dose using the equation (Aitken, 1985):

$$\mathrm{AD} = \frac{S_N - S_o}{S_{N+\beta} - S_{N'}} \times \beta \tag{7}$$

The applicability of this corrected form of Eq. (6) is discussed in the numerical results section.

6. Numerical results

6.1. Simulation results for the additive dose version of the predose technique

Fig. 3a shows the variations of the sensitivities S_0, S_N, $S_{N+\beta}$ with the paleodose PD, as calculated by the additive dose version of the predose technique. These three sensitivities vary linearly with the paleodose as shown in Fig. 3a, indicating that in principle the predose method should be accurate in this dose range. Fig. 3a also shows that the value of S_0 is about 50 times smaller than S_N, satisfying the requirement of "low-S_0" values for applicability of the predose technique. Fig. 3b shows the simulated glow curves obtained during the additive dose technique. The parameters used to obtain the simulation data in Fig. 3b are TD = 0.01 Gy, β = PD = 4 Gy.

Fig. 4a shows the simulated variation of the sensitivity S of the 110 °C TL peak with the added beta dose. Extrapolation of the fitted line to the x-axis gives the estimated accrued dose (AD) of the sample. Fig. 4b shows the results of the simulation for paleodoses in the range 0–4 Gy when using an activation temperature of T = 500 °C. The calibration dose β is taken to be equal to the paleodose, $\beta = PD$. Specifically, Fig. 4b shows the percent difference between the calculated accrued dose AD and the paleodose PD for three different values of the test dose. The bottom graph in Fig. 4b shows that the additive dose technique overestimates the paleodose received by the sample by 4–5% over the range of paleodoses PD = 0.2–2 Gy. Fig. 3a shows that for paleodoses larger than ∼ 1.5 Gy the sensitivities S_0, S_N and $S_{N+\beta}$ start exhibiting non-linear behavior, which leads to larger inaccuracies in the calculated AD.

The accuracy of the additive dose method is seen in Fig. 4b to decrease for low doses below ∼ 0.2 Gy, and the percent error approaches values larger than +10% at very small values of the paleodose. This decrease of the accuracy of the method at low paleodoses can be expected on physical grounds, since the test dose TD is of the same order of magnitude as the paleodose itself, and therefore administration of the TD can alter the distribution of electrons and holes in the nine energy levels of the Bailey model. This in turn leads to inaccuracies in the calculated accrued dose AD.

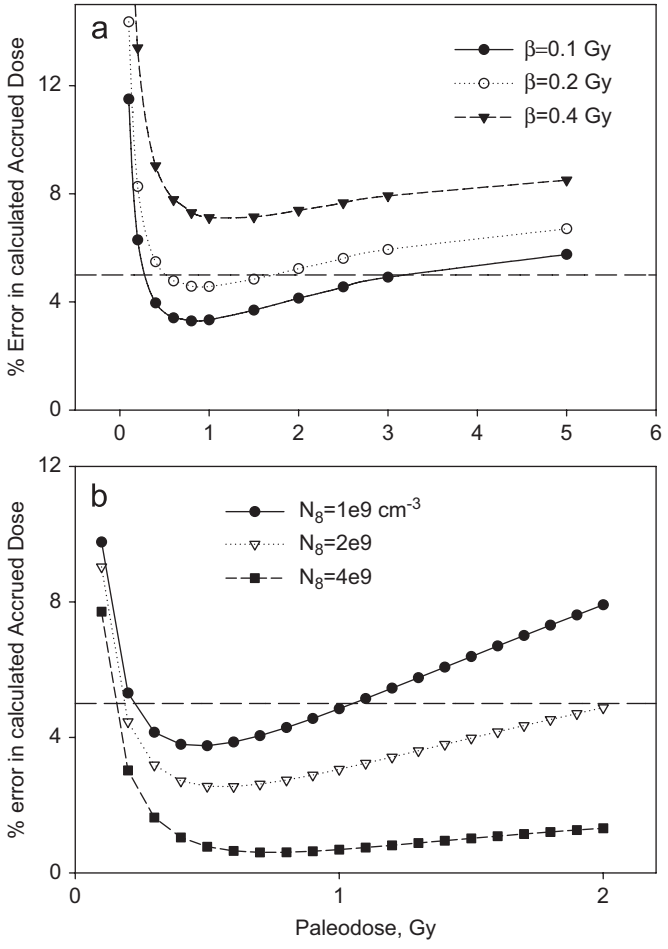

Fig. 5. (a) The effect of the calibration beta dose on the accuracy of the additive dose technique. A fixed test dose TD = 0.01 Gy and an activation temperature of 500 °C is used. (b) The effect of increasing the total concentration of holes in the luminescence center (N_8) on the accuracy of the additive dose technique.

One might also expect that the accuracy of the additive dose technique would be improved by using as small of a test dose as possible. Fig. 4b shows that the value of the test dose has a rather large effect on the accuracy, especially at low paleodoses. The results shown in Fig. 4b imply that in an experimental situation, the test dose should be made as small as possible, within the experimental constraints imposed by the magnitude of the smallest measurable TL signal.

Experimentally, it has been found that the results of the additive dose technique also depend of the calibration dose β given to the sample. Fig. 5a shows the variation of the accuracy of the simulation when the calibration dose is varied in the range β = 0.1–0.4 Gy, with a fixed test dose value of TD = 0.015 Gy. The data in Fig. 5a show that the accuracy of the simulation is improved at lower values of the calibration dose β. The results presented in this section for the additive dose technique are qualitatively similar to the ones obtained by Pagonis and Carty (2004) using the modified version of the model by Chen

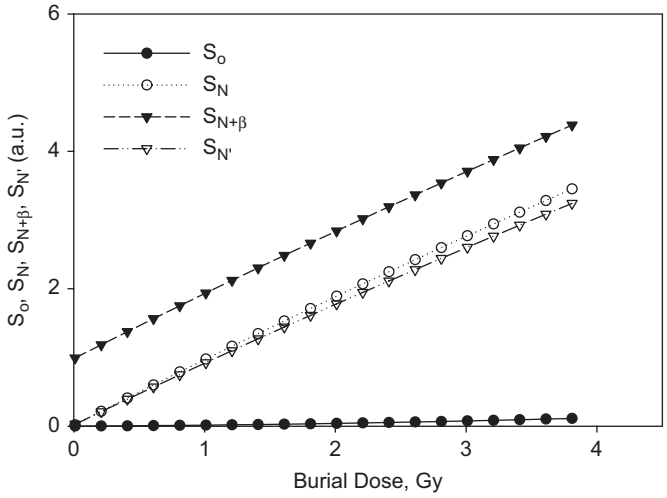

Fig. 6. Simulation results for the multiple activation version of the predose technique. The linear variations of the sensitivities S_0, S_N, $S_{N+\beta}$ with the paleodose PD, as calculated by the model in the range 0–4 Gy.

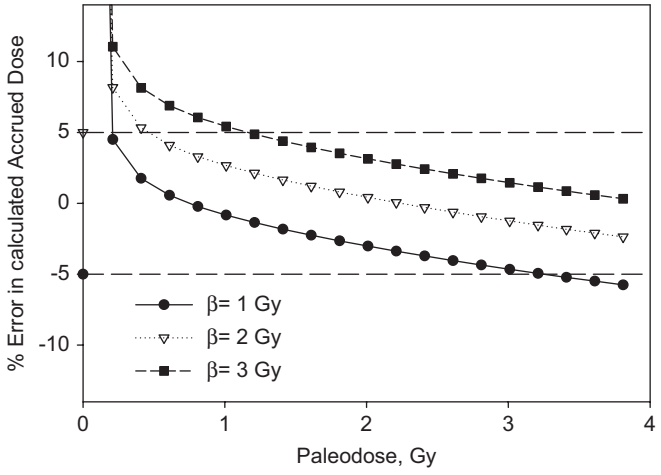

Fig. 7. The effect of the calibration beta dose on the accuracy of the multiple activation technique. A fixed test dose TD=0.015 Gy is used in this simulation.

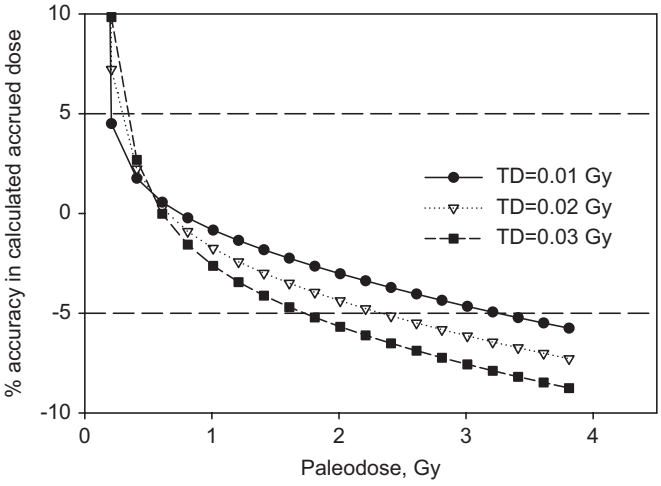

Fig. 8. The effect of the test dose TD on the accuracy of the multiple activation technique. A fixed calibration dose $\beta = 1$ Gy is used in this simulation.

and Leung (1998, 1999). As mentioned previously, one major improvement in the present work is presentation of the doses in appropriate units of Gy. Fig. 5b shows the effect of increasing the total concentration of holes in the luminescence center by factors of 2 and 4. It can be seen that the results of the additive dose method are rather sensitive to variations of the parameter N_8. The bottom curve in Fig. 5b showing that it is possible in some samples to reproduce the paleodose with an accuracy of a few percent in the extended dose range 0–4 Gy when using the additive dose technique.

6.2. Simulation results for the multiple activation version of the predose technique

Fig. 6a shows the variations of the sensitivities S_0, S_N, $S_{N+\beta}$ and $S_{N'}$ with the paleodose PD, as calculated by the multiple activation version of the predose technique. These four sensitivities are seen to vary linearly with the paleodose, indicating that in principle again the predose method should be accurate in this dose range. From the data of Fig. 6 it is seen that the radiation quenching ratio $S_{N'}/S_N \sim 0.90 < 1$. This compares well with the typical experimentally observed variation of the quenched sensitivity with the calibration dose, namely a $\sim 10\%$ reduction for every Gy of calibration dose (Aitken, 1985, p. 158).

Fig. 7 shows the results of the simulation for paleodoses in the range 0–4 Gy when using an activation temperature of $T = 500\,^{\circ}$C, and for three different values of the calibration dose $\beta = 1, 2, 3$ Gy. The simulation data in Fig. 7 and Fig. 5a shows that the multiple activation method is more accurate than the additive dose method under similar experimental conditions, and that it can estimate the paleodose with an accuracy of ± 1–5% for doses between 0.2 and 3 Gy. Fig. 8 shows the effect of the test dose on the accuracy of the multiple activation method. As seen in Fig. 8, using a larger test dose TD = 0.03 Gy results in a decreased range of 0.3–1.7 Gy for accurate dose determination.

A comparison between the accuracy of Eqs. (6) and (7) for the accrued dose within the multiple activation technique leads to the conclusion that the corrected Eq. (7) is more accurate for low paleodoses PD < 0.5 Gy, while for paleodoses larger than 0.5 Gy the uncorrected Eq. (6) gives better results. The actual differences between Eqs. (6) and (7) are typically a few percent. However, one cannot exclude the possibility that a different set of parameters in the model could lead to different conclusions concerning the accuracy of Eqs. (6) and (7).

Experimentally, it is found that some types of quartz exhibit enhancement instead of reduction of the sensitivity, i.e. the ratio $S_{N'}/S_N > 1$. Fig. 9a and b shows the simulated glow curves during the multiple activation method, for two different values of the concentration of holes N_8 in the sample, namely for the original value of $N_8 = 10^{11}\,\mathrm{cm}^{-3}$ in the Bailey model, and for a much smaller value of $N_8 = 10^{9}\,\mathrm{cm}^{-3}$. The data in Fig. 9a shows that in the case of "low-S_0" value (corresponding to $N_8 = 10^{9}\,\mathrm{cm}^{-3}$) the ratio $S_{N'}/S_N \sim 0.90 < 1$ and the

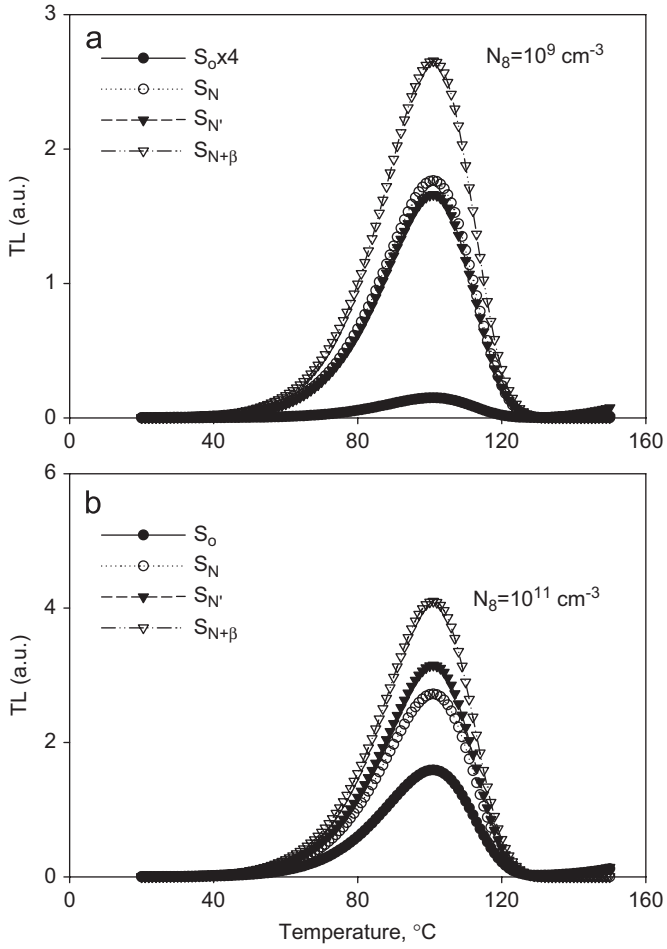

Fig. 9. Simulated glow curves during the multiple activation method, for two different values of the total concentration of holes N_8 in the luminescence center. (a) In the case of "low-S_0" value, the quartz sample exhibits radiation quenching $S_{N'} < S_N$. (b) In the case of "high-S_0" value, the sample exhibits radiation-enhanced sensitivity $S_{N'} > S_N$.

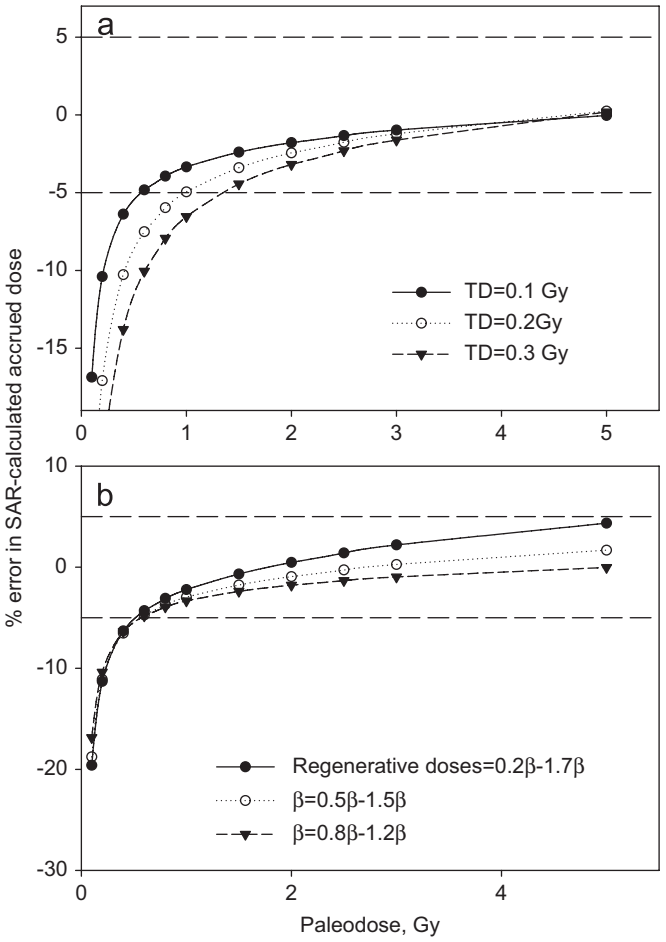

Fig. 10. The results of simulating the single aliquot regenerative protocol (SAR) using the same parameters as for the predose technique. The steps in the simulation are shown in Table 4. (a) The effect of the test dose TD on the accuracy of the OSL/SAR technique. (b) The effect of the chosen intervals of beta doses on the accuracy of the OSL/SAR technique.

quartz sample exhibits radiation quenching. On the other hand, Fig. 9b shows that in the case of "high-S_0" value (corresponding to $N_8 = 10^{11}\,\mathrm{cm}^{-3}$) the ratio $S_{N'}/S_N \sim 1.20 > 1$ and the quartz sample exhibits radiation-enhanced sensitivity. Close examination of the concentrations of the nine energy levels in the Bailey model during the simulations provides us with the following explanations of these opposite behaviors.

In the case of a "low-S_0" sample, electrons released from the "110 °C" TL trap during measurement of $S_{N'}$ are captured in the luminescence center L, resulting in a reduced instantaneous concentration n_8 of holes in L. A lower value of n_8 leads to a lower value of the observed TL signal according to Eq. (5), and hence to a reduced (quenched) activated sensitivity $S_{N'}$. In the case of the "high-S_0" value sample of Fig. 9b, the higher total concentration of holes in the luminescence center (N_8) leads to more holes being captured in the luminescence center during the natural irradiation of the sample according to Eq. (1). This leads to a higher concentration of holes n_8 during the measurement of $S_{N'}$, and hence to a higher value of the observed TL signal according to Eq. (5).

It is noted that two slightly different mechanisms for radiation quenching and radiation enhanced sensitivity than the ones suggested here were proposed previously by Aitken (1985), on a purely empirical basis. Within our kinetic simulations, these two phenomena are given a quantitative mathematical description.

We also studied the effect of increasing the concentration of holes in the luminescence center N_8, in a simulation similar to the one depicted in Fig. 5b for the additive dose method. The results of the corresponding simulation for the multiple activation technique were very similar to Fig. 5b and are not shown here. It is concluded that the results of the multiple activation technique are also rather sensitive to natural variations of the parameter N_8.

6.3. Simulation results for the OSL/SAR technique

Fig. 10a and b shows the results of simulating the popular and very successful single aliquot regenerative protocol (SAR) developed during the past 10 years (Wintle and Murray, 2006).

The steps in this simulation are shown in Table 4. The five regenerative doses used were 0.8β, β, 1.2β, 0 and 0.8β, and the test dose used was 0.1 Gy. The preheat temperature used in the SAR protocol simulation was 10 s at 260 °C for the regenerative dose measurements, and the cut-heat used for the test dose measurements was 20 s at 220 °C. The results of the SAR protocol showed good recycling ratio close to unity. The sensitivity corrected signals L/T were used to reconstruct the dose response curve, and as usual an interpolation was used for estimating the accrued dose by the sample.

Fig. 10a shows the results of the SAR/OSL simulation for paleodoses in the range 0–5 Gy, and for three different values of the test dose TD = 0.1, 0.2 and 0.3 Gy. The simulation data in Fig. 10a shows that the SAR technique is more accurate than both versions of the predose technique, estimating the paleodose with an accuracy of ±1–5% for doses between 0.3 and 5 Gy. Using a larger test dose results once more in a decreased range of accurate dose determination. Fig. 10b shows the results of the SAR simulation for three different choices of dose intervals used for the regenerative doses. There is a rather small decrease of the accuracy of the protocol when larger dose intervals are used. In general, the results of the simulations show that the SAR protocol is less sensitive to changes in the experimental conditions, than either the additive dose or the multiple activation predose techniques.

7. Conclusions

The Bailey model was used successfully in this paper to simulate the complete sequence of experimental steps taken during the additive dose and the multiple activation versions of the predose technique. This model contains a total of 44 kinetic parameters, while the simple 4-level model of Pagonis and Carty (2004) contained a total of just 13 kinetic parameters. Despite its simplicity, the 4-level model yielded similar results to the much more complex Bailey model for the case of the additive dose technique. The solution of the kinetic equations using both models elucidates the process of transfer of holes from the hole reservoirs to the luminescence center caused by the high temperature annealing. In addition, in this paper, it was shown that the Bailey model also provides a description of the mechanisms of radiation quenching and radiation-enhanced sensitization of the 110 °C TL peak in quartz. The simulation also yields the correct order of magnitude for these two important phenomena in quartz samples.

The empirical assumptions of linear dependence of S_0, S_N, $S_{N'}$ and $S_{N+\beta}$ on the paleodose are given a specific mathematical form, and are shown to lead to accurate estimates of the value of PD over a typical range of 0.2–2 Gy. Non-linear dependence of these sensitivities for paleodoses PD $> \sim 2$ Gy leads to inaccuracies in the calculated accrued dose.

The results of the simulations show that the SAR protocol which is based on optically stimulated signals, is in general less sensitive to the specific experimental conditions, than either the additive dose or the multiple activation techniques.

Acknowledgments

The financial support provided by Dr. Thomas Falkner, Provost and Dean of Faculty at McDaniel College, and of the Faculty Development Committee at McDaniel College are gratefully acknowledged.

References

Adamiec, G., Garcia-Talavera, M., Bailey, R.M., Iniguez de la Torre, P., 2004. Application of a genetic algorithm to finding parameter values for numerical stimulation of quartz luminescence. Geochronometria 23, 9–14.

Adamiec, G., Bluszcz, A., Bailey, R., Garcia-Talavera, M., 2006. Finding model parameters: genetic algorithms and the numerical modelling of quartz luminescence. Radiat. Meas. 41, 897–902.

Aitken, M.J., 1985. Thermoluminescence Dating. Academic, London.

Bailey, R.M., 2001. Towards a general kinetic model for optically and thermally stimulated luminescence in quartz. Radiat. Meas. 33, 17–45.

Bailey, R.M., 2004. Paper I—Simulation of dose absorption in quartz over geological timescales and its implications for the precision and accuracy of optical dating. Radiat. Meas. 38, 299–310.

Bailey, R.M., Smith, B.W., Rhodes, E.J., 1997. Partial bleaching and the decay form characteristics of quartz OSL. Radiat. Meas. 27, 123–136.

Bailiff, I.K., 1994. The pre-dose technique. Radiat. Meas. 23, 471–479.

Bailiff, I.K., 1997. Retrospective dosimetry with ceramics. Radiat. Meas. 27, 923–941.

Bailiff, I.K., Haskell, E.H., 1984. The use of the predose technique for environmental dosimetry. Radiat. Prot. Dosim. 6, 245–248.

Bailiff, J.K., Holland, N., 2000. Dating bricks of the last two millennia from Newcastle upon Tyne: a preliminary study. Radiat. Meas. 32, 615–619.

Bailiff, J.K., Bøtter-Jensen, L., Correcher, V., Delgado, A., Göksu, H.Y., Jungner, H., Petrov, S.A., 2000. Absorbed dose evaluation in retrospective dosimetry: methodological developments using quartz. Radiat. Meas. 32, 609–613.

Chen, R., 1979. Saturation of sensitization of the 100 °C TL peak in quartz and its potential application in the pre-dose technique. Eur. PACT J. 3, 325–335.

Chen, R., Leung, P.L., 1998. Processes of sensitization of thermoluminescence in insulators. J. Phys. D: Appl. Phys. 31, 2628–2635.

Chen, R., Leung, P.L., 1999. Modeling the pre-dose effect in thermoluminescence. Radiat. Prot. Dosim. 84, 43–46.

Chen, R., Pagonis, V., 2004. Modeling thermal activation characteristics of the sensitization of thermoluminescence in quartz. J. Phys. D: Appl. Phys. 37, 159–164.

Galli, A., Martini, M., Montanari, C., Panzeri, L., Sibilia, E., 2006. TL of fine-grain samples from quartz-rich archaeological ceramics: dosimetry using the 110 and 210 °C TL peaks. Radiat. Meas. 41, 1009–1014.

Göksu, H.Y., Stoneham, D., Bailiff, I.K., Adamiec, G., 1998. A new technique in retrospective TL dosimetry: pre-dose effect in the 230 °C TL glow peak of porcelain. Appl. Radiat. Isot. 49, 99–104.

Göksu, H.Y., Schwenk, P., Semiochkina, N., 2001. Investigation of the thermal stability of 210 °C TL peak of quartz and dating the component of terrazzo from the monastery church of Tegernsee. Radiat. Meas. 33, 785–792.

Haskell, E.H., 1993. Retrospective accident dosimetry using environmental materials. Radiat. Prot. Dosim. 47 (1/4), 297–303.

Haskell, E.H., Kaipa, P.L., Wrenn, M.E., 1988. Pre-dose TL characteristics of quartz inclusions removed from bricks exposed to fallout radiation from atmospheric testing at the Nevada test site. Nucl. Tracks Radiat. Meas. 14, 113–120.

Haskell, E.H., Bailiff, I.K., Kenner, G.H., Kaipa, P.L., Wrenn, M.E., 1994. Thermoluminescence measurements of gamma-ray doses attributable to fallout from the Nevada Test Site using building bricks as natural dosimeters. Health Phys. 66, 380–391.

Hütt, G., Brodksi, L., Bailiff, I.K., Göksu, Y., Haskell, E., Jungner, H., Stoneham, D., 1993. Accident dosimetry using environmental material collected from regions downwind of Chernobyl: a preliminary evaluation. Radiat. Prot. Dosim. 47, 307–311.

Itoh, N., Stoneham, D., Stoneham, A.M., 2001. The predose effect in thermoluminescent dosimetry. J. Phys.: Condens. Matter 13, 2201–2209.

Kitis, G., Pagonis, V., Chen, R., Polymeris, G., 2006a. A comprehensive study of the predose effect for three quartz crystals of different origin. Radiat. Prot. Dosim. 119 (1–4), 438–441.

Kitis, G., Pagonis, V., Chen, R., 2006b. Comparison of experimental and modelled quartz thermal-activation curves obtained using multiple-and single-aliquot procedures. Radiat. Meas. 41, 910–916.

Martini, M., Spinolo, G., Vedda, A., 1987. Defects dynamics in as-grown and electrodiffused quartz: an interpretation of the predose effect. J. Appl. Phys. 61, 2486–2488.

Pagonis, V., Carty, H., 2004. Simulation of the experimental pre-dose technique for retrospective dosimetry in quartz. Radiat. Prot. Dosim. 109, 225–234.

Pagonis, V., Kitis, G., Chen, R., 2003. Applicability of the Zimmerman predose model in the thermoluminescence of predosed and annealed synthetic quartz samples. Radiat. Meas. 37, 267–274.

Pagonis, V., Chen, R., Kitis, G., 2006. Theoretical modeling of experimental diagnostic procedures employed during predose dosimetry of quartz. Radiat. Prot. Dosim. 119 (1–4), 111–114.

Pagonis, V., Wintle, A.G., Chen, R., 2007a. Simulations of the effect of pulse annealing on optically-stimulated luminescence of quartz. Radiat. Meas. 42, 1587–1599.

Pagonis, V., Chen, R., Wintle, A.G., 2007b. Modelling thermal transfer in optically stimulated luminescence of quartz. J. Phys. D: Appl. Phys. 40, 998–1006.

Polymeris, G., Kitis, G., Pagonis, V., 2006. The effects of annealing and irradiation on the sensitivity and superlinearity properties of the 110 °C thermoluminescence peak of quartz. Radiat. Meas. 41, 554–564.

Stoneham, D., 1985. The use of porcelain as a low-dose background dosimeter. Nucl. Tracks 10, 509–512.

Wintle, A.G., Murray, A.S., 2006. A review of quartz optically stimulated luminescence characteristics and their relevance in single aliquot regeneration dating protocols. Radiat. Meas. 41, 369–391.

Yang, X.H., McKeever, S.W.S., 1988. Characterization of the predose effect using ESR and TL. Nucl. Tracks Radiat. Meas. 14, 75–79.

Zimmerman, J., 1971a. The radiation induced increase of the 100 °C TL sensitivity of fired quartz. J. Phys. C: Sol. Stat. Phys. 4, 3265–3276.

Zimmerman, J., 1971b. The radiation induced increase of the thermoluminescence sensitivity of the dosimetry phosphor LiF (TLD-100). J. Phys. C: Sol. Stat. Phys. 4, 3277–3291.